Fall 2021

Large extrusion bodies in Piwi family protein knockout strains in Tetrahymena thermophila

Jason Sasser
Western Washington University

Large extrusion bodies in Piwi family protein knockout strains in *Tetrahymena thermophila*

Jason Sasser

Abstract

The ciliate *Tetrahymena thermophila* encodes twelve distinct proteins of the PIWI family of small RNA binding proteins. Three of these *Tetrahymena* PIWI proteins (Twis) have previously been shown to be expressed in vegetative growth and bind predominantly to ~23-24 nucleotide (nt) small RNAs (sRNAs) (Couvillion et al., 2009). One of ~23-24 nt sRNA binding proteins, Twi2, is encoded by DNA sequence that has high sequence similarity to four other predicted Twi genes (Twis 3-6) which are normally not highly expressed. Using fluorescent microscopy imaging techniques, we examined mutant strains *TWI8Δ*, *TWI2-6Δ*, *TWI7Δ*, *TWI2-6/8Δ*, and *TWI7/8Δ* for accumulation of large extrusion bodies (EBs). EBs are nonnuclear DNA containing structures which are likely akin to mammalian micronuclei; these are structures commonly found as markers of genomic instability. We found no significant EB size increase in the strains *TWI2-6Δ* and *TWI7Δ* and a moderately enlarged EB phenotype in *TWI8Δ* cells compared to the reference parental strain SB210. *TWI2-6/8Δ* cells had the most exaggerated enlarged EB phenotype, suggesting that at least one of the five Twi proteins encoded by the *TWI2-6* gene cluster contributes to genome stability in addition to Twi8. *TWI7/8Δ* cells had highly variable EB area between replicates with the average EB being larger than that found in SB210, which may also implicate Twi7 in contributing to genome stability in absence of Twi8. Overall, these findings support a role for RNA interference (RNAi) in maintaining genome integrity in *Tetrahymena* that is dependent on Twi proteins.

Introduction

RNAi is a cellular mechanism in eukaryotes with various conserved functions including post-transcriptional silencing, heterochromatin formation, and genome defense against viruses and transposons (Matzke and Birchler, 2005, Gutbrod and Martienssen, 2020). The process of RNAi begins with the biogenesis of small RNA (sRNA). Generally, the sRNA biogenesis pathway involves the synthesis of double-stranded RNA (dsRNA) from single-stranded long non-coding RNA (lncRNA) by an RNA-dependent RNA polymerase (RdRP) which is then processed into sRNA by endoribonucleases DICER and DROSHA (Gutbrod and Martienssen, 2020). These sRNAs are thought to typically function in “effector” complexes with proteins of the PIWI/Argonaute family. This protein superfamily is characterized by the presence of a PIWI (p-element induced wimpy testis) domain and is conserved throughout all domains of life. In eukaryotes, PIWI/Argonaute proteins bound to a sRNA are guided to bind RNA with sequence complementarity with the sRNA. Interestingly, some prokaryotic PIWI proteins have been found to target DNA with an RNA guide, although this has not been observed in eukaryotes (Swarts et al., 2014). The first discovered function of RNAi, post-transcriptional silencing, uses this RNA targeting mechanism to trigger the degradation of mRNA transcripts. Since this initial discovery, many functions of RNAi have been found that contribute to maintaining genome integrity. These include heterochromatin formation around the centromeres, which contributes to proper chromosome segregation during mitosis, and

defense against transposons and viruses, which is the proposed ancestral function of RNAi. Along with these roles, RNAi factors and sRNAs have increasingly been reported to have functions in DNA damage response and repair pathways. Damaged-induced small RNA (diRNA) has been observed in model systems such as the insect *Drosophila melanogaster,* the fungus Neurospora crassa, the plant *Arabidopsis thaliana*, and cultured mammalian cells to be produced at the site of double-strand breaks (DSBs) to promote DSB repair by aiding the recruitment of DSB repair proteins (Gutbrod and Martienssen, 2020).

Tetrahymena thermophila is an understudied unicellular eukaryotic model organism with distinct scientific advantages for cellular and molecular studies. As a ciliate, they are part of the alveolate group of the stramenopile alveolate rhizaria (SAR) lineage, which makes them evolutionarily distant from common model organisms of the opisthokont lineage. This makes *Tetrahymena* an excellent model organism for exploring highly conserved eukaryotic features such as RNAi, while also providing opportunities to uncover evolutionarily innovative biology that is underappreciated or unknown. Like all ciliates, *Tetrahymena* exhibits nuclear dimorphism: it contains a large somatic nucleus called the macronucleus (MAC) and a smaller germline nucleus called the micronucleus (MIC). All gene expression in *Tetrahymena* comes from the MAC; the MIC is transcriptionally silent and solely functions for sexual reproduction via conjugation. During the vegetative *Tetrahymena* cell cycle, cells reproduce asexually. During cell division, the chromosomes of the MAC undergo amitosis (random segregation of chromosomes) enclosed in the nuclear membrane while the chromosomes in the MIC undergo enclosed mitosis. Interestingly, the MAC maintains a chromosome copy number of ~45; it is not currently understood how this ploidy is maintained despite chromosomes undergoing random segregation (Ruehle et al., 2016). It has been observed that during amitosis, chromatin globules form that contain DNA content similar to the full macronuclear genome, which has led to the proposal that these "macronuclear genome units" ensure that each of the daughter cell MACs receive balanced copies of each MAC chromosome (Endo and Sugai, 2011). When cultured under starvation conditions, pairs of sexually mature *Tetrahymena* of complementary mating types will undergo a sexually reproductive phase of the life cycle called conjugation. Conjugating cells exchange haploid nuclei created by meiosis of the diploid MICs to form zygotic MICs. While the parental MACs are eliminated, the zygotic MICs undergo mitosis and one mitotic copy serves as the genomic source material for the progeny MAC genome. Maturation of the progeny MAC involves developmentally programmed DNA elimination that removes most of the repetitive DNA in the zygotic MIC, including transposons and centromeres. The remaining DNA is processed into smaller minichromosomes, which undergo multiple rounds of replication to achieve a copy number of ~45 (Ruehle et al., 2016).

In *Tetrahymena thermophila*, one of the two known RNAi pathways generates ~27-30 nucleotide small RNAs called "scan(scn)RNAs" which function in the above-described process of developmentally programmed DNA elimination. Large RNA transcripts are produced from the MIC during prophase of meiosis and processed by "DICER-like" protein Dcl1 into scnRNA. These scnRNAs are transported into the cytoplasm where they are bound by a Twi protein, Twi1, which is not normally expressed in vegetative growth but becomes strongly expressed during conjugation. In addition, a second wave of scnRNAs are produced later during conjugation which bind to both Twi1 and Twi11, which are expressed during late

conjugation. The Twi-bound scnRNAs enter the parental MAC and scnRNAs that correspond to macronuclear DNA sequences are degraded. This leaves only scnRNAs corresponding to MIC-limited sequences, which includes repetitive DNA, centromeres, and transposons, which are transported to the developing MAC, in which they guide elimination of matching DNA sequences (Rzeszutek et al., 2020, Noto et al., 2015).

After the discovery of the ~27-30 nucleotide scnRNA RNAi pathway, it was found that *Tetrahymena* contain a separate ~23-24 nucleotide RNAi pathway that is expressed both in vegetative and conjugative growth (Lee and Collins, 2006). The biogenesis of these sRNAs is thought to begin with single-stranded non-coding RNA transcripts (ncRNA) which are generated from various genomic loci, including residual repetitive DNA presumably missed by DNA elimination during MAC maturation and regions predicted to yield unusually structured transcripts. These transcripts are transformed into dsRNA by RNA-dependent RNA polymerase complexes (RDRCs). RDRCs are protein complexes containing the RNA-dependent RNA polymerase Rdr1, one of two ribonucleotidyl transferases Rdn1 and Rdn2, and one of two additional subunits, Rdf1 and Rdf2, which are only present in RDRCs containing Rdn1 (Lee, et al., 2009). Accumulation of ~23-24 nucleotide sRNAs is also dependent on RNA silencing protein 1 (Rsp1), although it is currently unknown what molecular role Rsp1 plays in the biogenesis pathway (Talsky and Collins, 2012). The resulting dsRNA is processed by the *Tetrahymena* Dicer Dcr2 into ~23-24 nucleotide sRNAs which are bound predominantly by Twi proteins during vegetative growth (Couvillion et al., 2009).

Previous research has examined phenotypes of mutant strains lacking sRNA biogenesis proteins. Of the biogenesis mutants, strains fully lacking Rdr1, Rdn1, and Dcr2 could not be created, indicating that these proteins are necessary for cell viability (Lee et al 2021). In contrast, the mutant strains *RDN2Δ*, *RDF1Δ*, *RDF2Δ*, and *RSP1Δ* were successfully created. Of these, recent results in our group revealed that *RDN2Δ* and *RSP1Δ* have very large extranuclear DNA bodies compared to wildtype strain SB210 (Fig. 1, Lee et al., 2021). These are likely to be structures called chromatin extrusion bodies (EBs) in *Tetrahymena*.

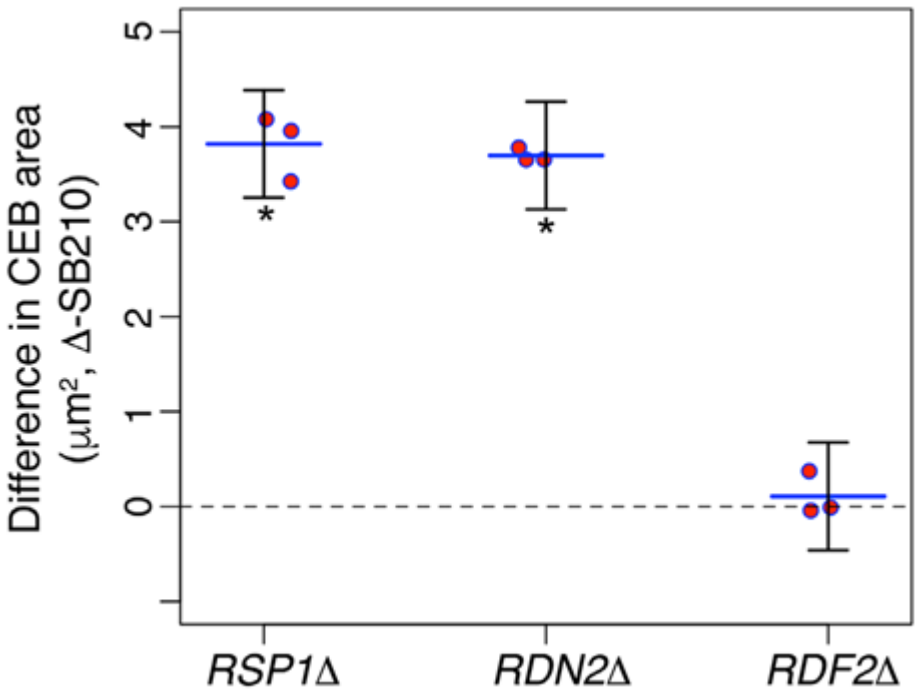

Figure 1. (From Lee et al., 2021) Difference in EB area from SB210 for RDRC knockout strains *RSP1Δ*, *RDN2Δ*, and *RDF1Δ*. Blue bars represent the overall average for each strain, while the red points represent the averages of individual replicates. Error bars represent a 95% confidence interval around the average. *p-value < 5x10^-7 based on a two way ANOVA.

EBs in *Tetrahymena* have been suggested to play a role in maintaining chromosome copy number due to the observation of large EBs in cells with induced over-replication (Kaczanowski et al., 2018), but have also been observed in cells with disruption to DSB repair (Marsh et al., 2000, Song et al., 2007). In addition, EBs bear similarity to mammalian micronuclei, which are commonly used as a marker of genotoxic stress and genetic instability. In mammalian cells, micronuclei are formed when nuclear envelope forms around lagging chromosomes or acentric chromosome fragments during mitosis. Formation of micronuclei can also occur through a poorly understood phenomenon of nuclear "blebbing". Micronuclei formation can be the result of either impaired DNA segregation or impaired DNA repair (Krupina et al., 2021). *Tetrahymena* EBs are thought to form in an analogous way; in *Tetrahymena* cells induced to form large EBs, "central granules" of chromatin have been observed in the MACs of cells preparing to divide (Kaczanowski et al., 2018). These are believed to ultimately segregate from the new MACs to form EBs. The similarity to mammalian micronuclei as well as observations of EBs in cells with disrupted DNA repair suggest that the large EBs observed in *RDN2Δ* and *RSP1Δ* cells may be indicative of DNA damage. Consistent with enlarged EBs reflecting elevated DNA damage and damage responses in *Tetrahymena RDN2Δ* and *RSP1Δ* during vegetative growth, gene ontology analysis of differentially expressed genes in these two strains found upregulation of genes with roles in DNA replication stress response, DNA damage response and DNA repair. Western blot and immunofluorescent staining analysis additionally revealed an increase in the levels of γ-H2A.X, a phosphorylated histone marker of DNA double stranded breaks, and Rad51, a

double stranded break repair protein associated with homologous recombination, in the MACs of both *RDN2Δ* and *RSP1Δ* (Lee et al., 2021). Together these findings suggest a role for the *Tetrahymena* ~23-24 nucleotide RNAi pathway in maintaining macronuclear genome integrity. These observations in strains lacking RNAi biogenesis machinery made us interested in investigating strains lacking *TWI* genes for EB phenotypes.

An important question following the characterization of the nonessential RNAi biogenesis machinery is whether the suggested role in maintaining genome integrity is dependent on sRNA-bound Twi effector complexes in *Tetrahymena,* and, if so, which Twi proteins are involved. Previous research has shown that Twi2, Twi8, and Twi12 are robustly expressed during vegetative growth, while Twi7 is also expressed during vegetative growth to a lesser extent (Couvillion et al., 2009). Of these proteins, Twi2 and Twi8 were found to copurify predominantly with ~23-24 nt sRNA, while Twi7 copurified with both 23-24 nt sRNA and a larger class of sRNA. Twi12 does not appear to bind 23-24 nt sRNA. Of the ~23-24 nt sRNA binding Twis robustly expressed during vegetative growth, overexpressed Twi8-GFP localizes to the MAC, while Twi2-GFP is distributed throughout the cytoplasm and appears to be excluded from the MAC (Fig. 2, Couvillion et al., 2009). This made Twi8 our most interesting candidate to investigate for a role in maintaining genome integrity. The genes encoding Twis 2, 3, 4, 5, and 6 are present in an uninterrupted tandem array (*TWI2-TWI6).* Of these, only *TWI2* was found to be expressed in vegetative growth or during conjugation. The genes *TWI3-TWI6* have high sequence similarity to *TWI2*, and a transcript was observed in *TWI2Δ* which likely originated from *TWI4*, the gene with the highest sequence similarity to *TWI2* (Couvillion et al., 2009). It is unknown whether an expected *TWI4* protein would bind ~23-24 nt sRNA and if the other *TWI*s in the tandem array would be expressed in cells lacking both *TWI2* and *TWI4*.

In this study, we chose to investigate EB frequency and size in various *TWI* knockouts gene knockouts strains. Previous work found evidence of DNA damage in cells lacking *TWI8* in the form of elevated RAD51 and increased size and number of RAD51 and *γ-H2AX* foci in the MAC compared to SB210. In contrast, *TWI2Δ* cells appeared to have slight RAD51 elevation, but not to an extent that was statistically significant (Lee et al., 2021). This suggests that at least *TWI8* is likely to be involved in maintaining genome integrity. Our study extends this previous work by investigating EB area as a marker of DNA damage. Based on previous results indicating DNA damage in *TWI8Δ* similar to *RDN2Δ* and *RSP1Δ*, we expected to see a similar elevation EB frequency and size. Additionally, we considered that although *TWI2Δ* did not previously show significant signs of DNA damage, this could be due to other genes in the *TWI2-TWI6* gene cluster being expressed to produce Twi2-like Twis in the absence of *TWI2* and does not necessarily indicate that Twi2 does not contribute to maintaining genome integrity. In order observe whether Twi proteins from the *TWI2-TWI6* cluster contribute to maintaining genome integrity, we choose to investigate EB phenotype in *TWI2-6Δ* cells. We also considered the possibility that another of the ~23-24 nt sRNA binding, vegetatively expressed Twis could contribute to maintaining genome integrity in the absence of Twi8, which led us to investigate strains *TWI2-6/8Δ* and *TWI7/8Δ* in addition to *TWI2-6Δ*, *TWI7Δ*, and *TWI8Δ*.

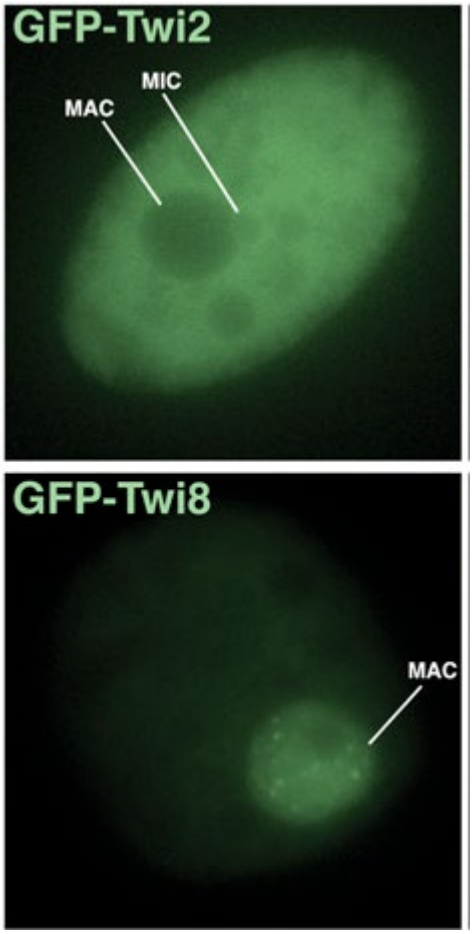

Figure 2. (From Couvillion et al., 2009) Strains overexpressing GFP tagged Twi2 and Twi8 under the control of cadmium-induced MTT1 promoter.

Results

To examine the EB phenotype of our *TWI* knockout strains we imaged four to seven biological replicates of *TWI2-6Δ, TWI7Δ, TWI8Δ, TWI2-6/8Δ, and TWI7/8Δ* paired with the parental reference strain SB210 and *RDN2Δ* as a positive control. Past results showed both an increase in EB size and number of cells with EBs in *RDN2Δ* compared to SB210 (Lee et al., 2021). Consistent with these previous findings, *RDN2Δ* had an odds ratio for EB positive cells of ~2.4 compared to SB210 – meaning that *RDN2Δ* cells were over two times more likely to have EB positive cells than SB210. Due to this, we anticipated that we would see similar results in at least some of our strains lacking *TWI* proteins. Surprisingly, we did not see an increase in the number of cells with EBs in any of our strains lacking *TWI* proteins, but instead saw a significant decrease for *TWI7Δ* and *TWI8Δ* cells based on a generalized linear model (values that were less than 1 in the odds ratio reported in Table1). Additionally, the percentage of EB positive cells varied greatly between biological replicates within most of the strains. For example, SB210 ranged from 3-35 percent of cells with EBs over eight biological replicates.

Genotype	**SB210**	***RDN2Δ***	***TWI2-6Δ***	***TWI7Δ***	***TWI8Δ***	***TWI2-6/8Δ***	***TWI7/8Δ***
Number of Replicates	9	7	4	4	7	5	5

Average EB+ cells across all replicates (%)	21	36	28	6	15	25	16
Range of EB+ cells (%)	3-35	21-50	16-37	5-8	8-31	21-33	11-25
odds Ratio (Δ/SB210)		2.4	1.1	0.4	0.7	1	1.2
p-value		<2e-16 *	0.345	1.08e-16 *	7.21e-06 *	0.932	0.173

Table 1. Percent of EB positive cells. Odds ratio represents the probability of finding an EB positive cell compared to the probability of finding an EB positive cell in SB210. *p-value < 1e-05

Interestingly, while number of cells with EBs was not elevated in any of our *TWI* knockout strains, average EB size did show elevation in a pattern that was strongly consistent with independent RAD51 Western blotting results for the same strains (EB area analysis shown in Figure 4 and Western blotting by Courtney Yoshiyama, personal communication). Of our *TWI* knockout strains, *TWI2-6/8Δ* had the largest elevated EB area phenotype, with an average area across five biological replicates that was significantly larger than our reference strain SB210 and slightly larger than our positive control, *RDN2Δ* (p-value of 0.0953 from an ANOVA and Tukey test comparison of *TWI2-6/8Δ* - *RDN2Δ)*. In comparison, *TWI8Δ* appeared to have moderately larger EBs than SB210 ($p < 0.15$), while *TWI2-6Δ* had no significant EB area elevation ($p = 0.789$, Fig. 4A). While EB area for replicates with a high number of measurable EBs generally appear to fit a normal distribution, those with the largest average EB areas, such as *RDN2Δ* and *TWI2-6/8Δ,* tend to be somewhat skewed towards larger EBs due to a small number of extremely large EBs (Figures 4B, 4C). Of our knockouts, *TWI7/8Δ* had the greatest variability in EB size between replicates and overall had a significantly larger EB phenotype than SB210 despite two replicates having about the same average EB area as SB210 (Figure 4A). Distribution patterns within *TWI7/8Δ* replicates had similar variation: the replicates with larger average areas were skewed towards larger EBs by a few very large EBs, while those that had similar area to SB210 had a tighter, more symmetrical distribution (Figure 4C). In contrast, *TWI7Δ* showed very little variation across four replicates and consistently had EB areas similar to SB210 (Figures 4A, 4C).

A.

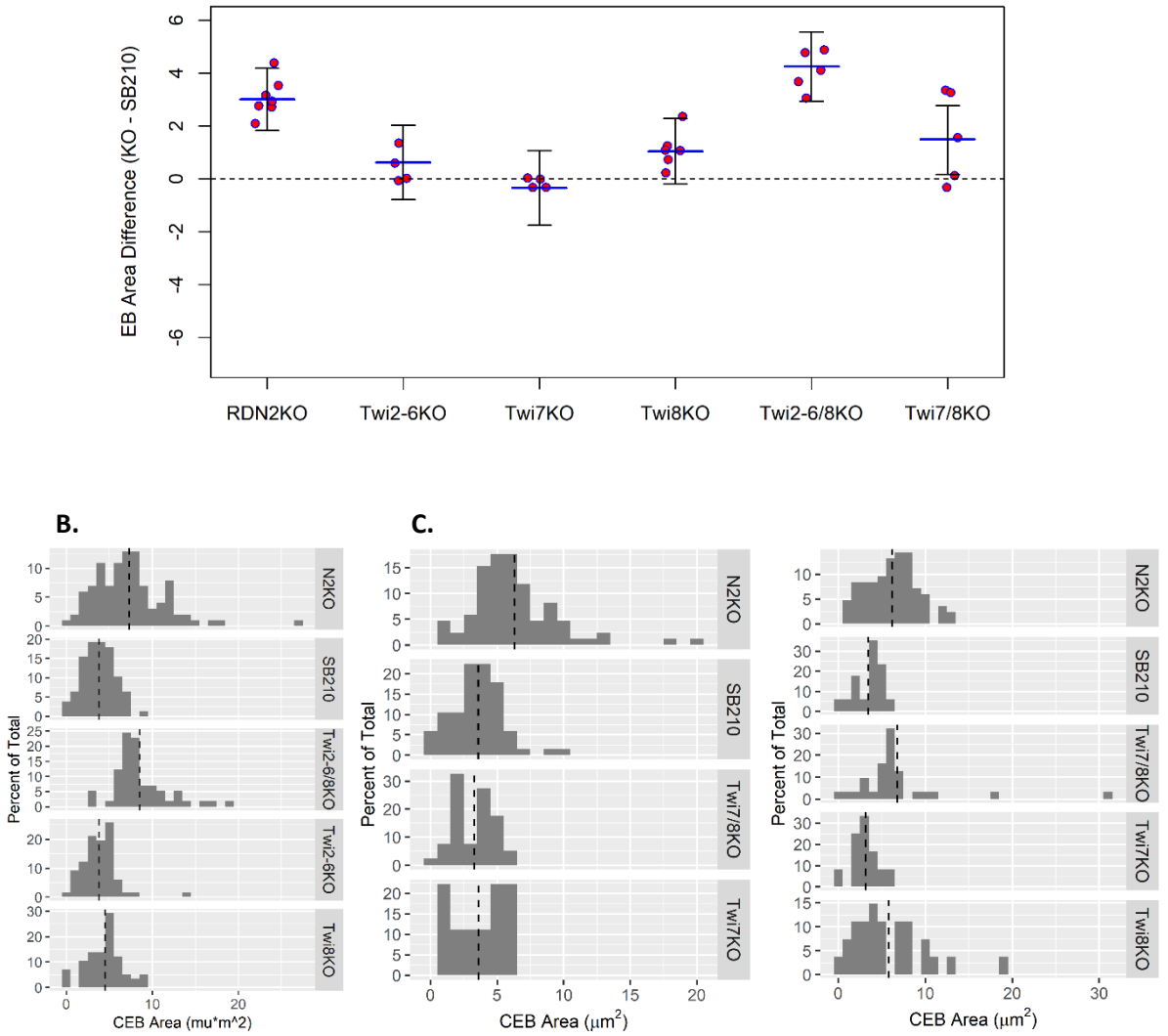

Figure 3. EB area. (A) Average EB area difference (KO-SB210) across biological replicates. Blue bars represent the overall average for each strain, while the red points represent the averages of individual replicates. Statistics were generated using ANOVA and TukeyHSD test. P-values: *RDN2Δ* = 3x10^-6, *TWI2-6Δ* = 0.789, *TWI7Δ* = 0.923, *TWI8Δ* = 0.142, *TWI2-6/8Δ* < 1x10^-6, and *TWI7/8Δ* = 0.021. (B) Histograms displaying percent distribution of EB area for *RDN2Δ, SB210*, *TWI2-6/8Δ, TWI2-6Δ,* and *TWI8Δ* in a representative replicate. Average area for each strain is represented as a dashed vertical line. (C) Similar histograms as (B) with *TWI7Δ* and *TWI7/8Δ* instead of *TWI2-6Δ* -and *TWI2-6/8Δ*. On the left is a replicate in which *TWI7/8Δ* EB area did not differ from SB210, while on the right is a replicate in which *TWI7/8Δ* had elevated EB area.

Discussion

Strains which showed elevated EB area also showed elevated levels of Rad51 (C. Yoshiyama, data not shown) in a highly consistent pattern (*TWI2-6/8Δ* > *RDN2Δ* > *TWI8Δ*). Due to this, we suspect that EB area is indicative of genome instability. Of strains *TWI2-6Δ*, *TWI7Δ*, and *TWI8Δ*, only *TWI8Δ* presented an elevated EB area phenotype. This suggests that Twi8 is the primary ~23-24 nt sRNA protein which plays a role in protecting genome integrity. This

finding makes sense given that Twi8 is the only one of these Twi proteins that has been shown to localize to the MAC, though Twi3, 4, 5, and 6 are not expressed to any substantial level during vegetative growth and localzation of the modestly expressed Twi7 has not been examined However, removal of *TWI8* alone was not enough to generate the same extent of enlargement of EBs that has been seen in strains lacking sRNA biogenesis proteins Rdn2 and Rsp1. We hypothesize that this could be due to at least one of the other ~23-24 sRNA binding Twis rescuing the lost function of Twi8 when it is missing or otherwise compromised in maintaining genome integrity. From our results, *TWI2-6/8Δ* had the largest EB area phenotype. Because *TWI2* is the only gene that is highly expressed during vegetative growth from the uninterrupted tandem array containing *TWI2-6,* we suspect Twi2 is the most likely candidate to rescue genome integrity in the absence of Twi8. It is also possible that Twi7 could play a similar role, although more replicates of *TWI7/8Δ* should be done due to the observed inconsistency between *TWI7/8Δ* replicates. It is worth noting that the three *TWI7/8Δ* replicates which show elevated EB area were cultured from the same set of cells maintained during a particular period of time, while the two replicates which show no elevated EB area were from two separate sets of cells maintained at two different times. It is possible that if contamination occurred during cell passaging during maintenance, it could have resulted in the elevated area we see in these three replicates. However, we have no other reason to believe that contamination did occur, and it is equally possible that these results are due to natural biological variation. Further replicates should be done to see if EB area continues to vary, or if it matches SB210.

Future Directions

Future studies in our lab will be centered on determining *how* the ~23-24 nt sRNA RNAi pathway is involved in maintaining genome integrity and further narrowing down which Twis are involved. Twi protein localization can be investigated via immunofluorescent confocal and widefield microscopy to examine if Twi8 forms subnuclear foci in the MAC that line up with foci of RAD51 and the double-stranded break associated histone marker *γ-H2AX.* This will allow us to determine if Twi8 is being recruited to sites of double stranded breaks, which would support a role in the DNA damage response, as opposed to a protective role to prevent DNA damage in the first place. Additionally, co-immunoprecipitation of Twi8 to see which proteins it may complex with could help to reveal its specific molecular function.

Our working hypothesis is that Twi2 rescues some of the lost function of Twi8 in maintaining genome integrity. Twi2 is known to localize to the cytosol in unmutated reference cell strains, but the localization pattern of Twi2 in *TWI8Δ* remains to be seen. Based on our hypothesis, we would expect that in *TWI8Δ* cells, Twi2 would localize to the MAC. Additionally, we do not know if Twi2 is the only Twi protein contributing to maintaining genome integrity from the *TWI2-6* tandem repeat in our *TWI8Δ* cells. We hope to test this by investigating *TWI2/8Δ* and *TWI2/4/8Δ* strains for DNA damage phenotypes, including EB frequency and area.

In addition to the Twi proteins involved in maintaining genome integrity, we are interested in investigating candidate loci in the *Tetrahymena* genome at which DNA damage may occur. DNA damage in the absence of protective Twis may occur on two classes of sRNA genomic precursors: pseudogene clusters and high-copy repeats. Sequenced ~23-24 nt sRNA that map to

the predicted open reading frames of pseudogene loci in the *Tetrahymena* genome bind to Twi2, Twi7, and Twi8; and accumulate in a manner dependent on Rdn2 and Twi2. Additionally, some of the~23-24 nt sRNA mapped to high-copy repeats: tandem arrays of ~150 bp units repeated to span 2-20. High-copy repeat derived sRNA also bound Twi2, Twi7, and Twi8. Accumulation of high-copy repeat sRNA was reduced by knockout of individual RDRC proteins and *TWI2* and was dependent on Twi8 (Couvillion et al., 2009). It is possible that DNA damage could occur at these repetitive DNA loci, which are some of the few repetitive elements left in the MAC after developmentally programmed DNA elimination. It is also interesting to note again that *TWI2/8Δ* had somewhat higher elevated EB area compared to *RDN2Δ* (p-value = 0.953). This could be because high-copy repeat derived sRNA still accumulate in the absence of *RDN2Δ*, but presumably neither pseudogene cluster nor high-copy repeat derived sRNA would accumulate in the absence of both Twi2 and Twi8.

In order to better understand the role the ~23-24 nt sRNA RNAi pathway plays in genome integrity, it will also be beneficial to investigate the manner of formation and consequences of EBs. As previously mentioned, EBs are believed to form from lagging chromosomes or chromosome fragments that do not segregate into either of the new MACs during amitosis. Micronuclei in mammals are similarly known to form from lagging chromosomes due to factors such as malfunctioning centromeres and acentric chromosomes resulting from DNA double-stranded breaks (Krupina et al., 2021); however, these causes are centromere dependent, and the MAC of *Tetrahymena thermophila* lacks centromeres. Past research has indicated that EBs form in a "center granule" of chromatin which is isolated in the center of the amitotically dividing MAC by microtubules (Kaczanowski et al., 2018), but it is unknown whether this process randomly excludes chromatin, or if it is more selective. It could be that the formation of EBs functions to exclude damaged chromatin which DNA repair processes failed to repair. If this turns out to be the case, it would indicate that the EB phenotype which we observed in strains such as *TWI2-6/8Δ* formed due to an impaired DNA damage response. It is also possible that DNA damage is occurring because of a disruption to normal DNA replication, as RNAi has been proposed to regulate DNA copy number in *Oxytricha*, another ciliate model organism (Khurana et al., 2018). Alternatively, EBs could be a driver of DNA damage in our knockout strains. In mammals, micronuclei are known to drive DNA damage via a process known as chromothripsis. In a chromothriptic event, the DNA present in mammalian micronuclei shatters and is then reincorporated into the nucleus, where the fragmented DNA undergoes aberrant reassembly (Krupina et al., 2021). If this occurs with EBs as well, it is possible that the large EBs in our knockout strains could form as a result of impeded chromosome segregation and that DNA damage results from these EBs. This would suggest that rather than having a role in DNA damage response, it could be that the ~23-24 nt sRNA pathway has a role in chromosomal segregation during amitosis. Understanding the direction of the relationship between EB and DNA damage is important to understanding the role of the ~23-24 nt sRNA pathway in maintaining genome integrity. Studying this pathway will help contribute to the growing awareness of the role of RNAi factors and sRNAs in maintaining genome integrity in diverse eukaryotes.

Methods

Culturing and strain maintenance

Tetrahymena strains were revived from liquid nitrogen or slow growing soy stocks every 1-2 months and passaged every 4-5 days in 24-well plates. Experiments were initiated with 5 mL cultures and grown at 30° C, shaking at 125 rpm, for 16-18 hours or until cells reached mid-log density (~2-4 x 10^5). Cells were counted using a hemacytometer. Growth media was made with 2% proteose peptone, 0.2% bacto-yeast extract, 12 µM FeCl, 0.2% glucose, 250 µg/ml ampicillin and streptomycin, and 1.25 µg/ml amphotericin B.

Immunofluorescent staining

Cells were fixed in 2% paraformaldehyde in 2x PBS and stored in 1x PBS for no more than 24 hours or used immediately. Cells were dried on microscope cover-slips, then permeabilized in 0.1% Triton X-100 in 1x PBS. Blocking was done with 5% BSA in PBS + 0.05% Tween-20 (PBS-T). Cells were probed with 1:5000 α-pH3S10 (primary antibody, labels mitotic MICs), washed in PBS-T, then stained with 1:1000 DAPI and 1:1000 goat anti-rabbit Alexa Fluor 568 (secondary antibody). For each position, cells were imaged with a z-stack of ~20 µm slices in the DIC (transmitted light), DAP (green), CHE (red), and GFP (blue) channels (GFP channel was used for visualization of autofluorescence). EBs were identified as structures within the cell that appeared in the DAP channel but did not fluoresce in CHE or GFP channel, excluding the MAC and MIC. MICs were distinguished by EBs by either the mitotic MIC stain (pH3S10) or it was assumed at every cell lacking a mitotic MIC possessed one MIC located near the MAC. EBs were manually counted and marked on ImageJ. Cells were not counted or marked if they lay partially outside of the field of view of the image, or if they appeared damaged (for example, cells with a torn membrane were not counted). EB areas were measured using a semiautomated ImageJ code. Occasionally the code would fail to distinguish the EB from nearby fluorescent bodies, often the MAC, or would fail to measure the entire EB, presumably due to the EB being to small or faint for the code to distinguish. These measurements made up around 20% of the EBs marked on average and were omitted from area quantification analysis.

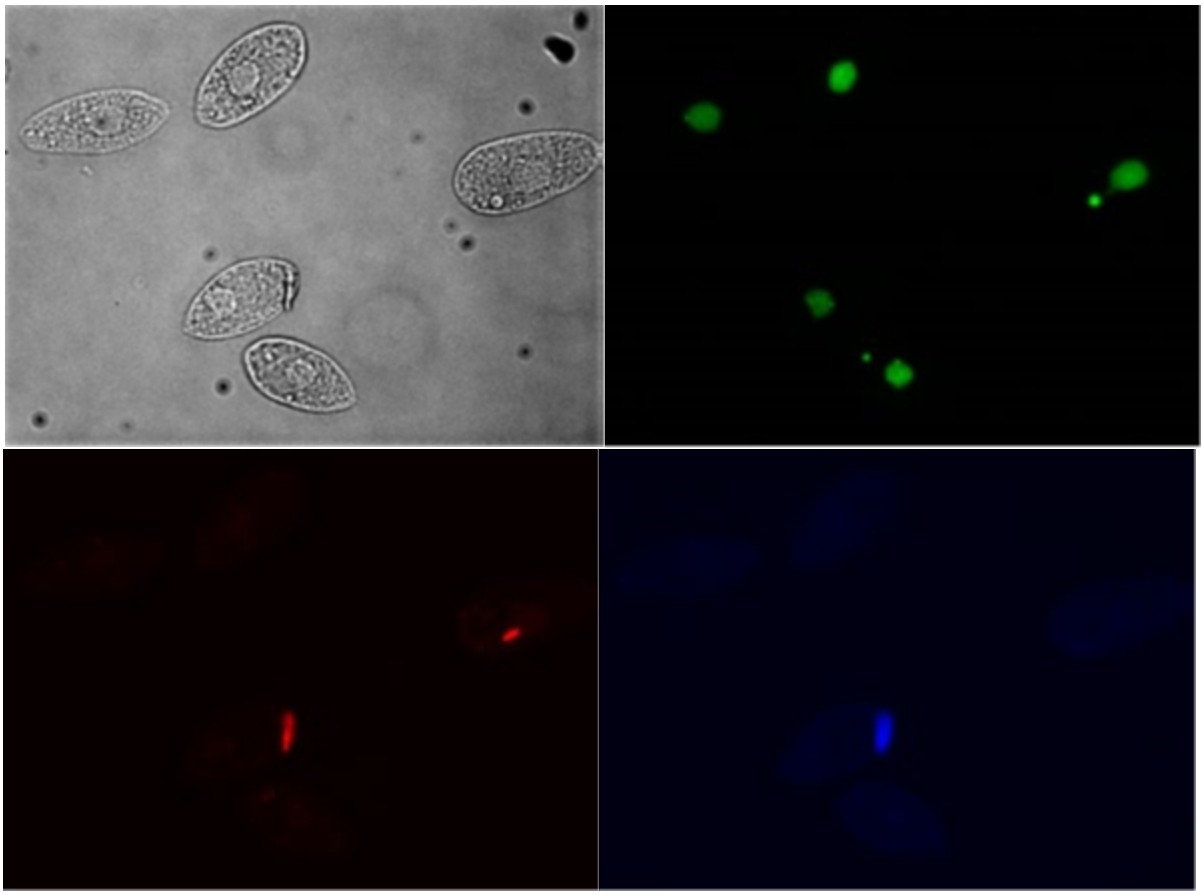

Figure 4. Image of *TWI2/8Δ* cells in all channels. Green channel shows DAPI staining. EBs indicated by yellow arrows. Red channel shows α-PH3S10 staining of mitotic MICs. Blue channel shows autofluorescence.

Imaging and EB quantification

Images were acquired on a Leica DMi6000 microscope with a Leica HCX 40× Plan Fluor 0.6 NA objective and Leica DFC3000G CCD camera using the LASX software. Images were taken to include ~200-300 healthy looking, clearly visible cells per biological replicate for each strain.

References

Couvillion MT, Lee SR, Hogstad B, Malone CD, Tonkin LA, Sachidanandam R, Hannon GJ, Collins K. Sequence, biogenesis, and function of diverse small RNA classes bound to the Piwi family proteins of Tetrahymena thermophila. Genes Dev. 2009 Sep 1;23(17):2016-32. doi: 10.1101/gad.1821209. Epub 2009 Aug 5. PMID: 19656801; PMCID: PMC2751968.

Endo M, Sugai T. Amitotic division of the macronucleus in Tetrahymena thermophila: DNA distribution by genomic unit. Zoolog Sci. 2011 Jul;28(7):482-90. doi: 10.2108/zsj.28.482. PMID: 21728796.

Gutbrod MJ, Martienssen RA. Conserved chromosomal functions of RNA interference. Nat Rev Genet. 2020 May;21(5):311-331. doi: 10.1038/s41576-019-0203-6. Epub 2020 Feb 12. PMID: 32051563.

Khurana JS, Clay DM, Moreira S, Wang X, Landweber LF. Small RNA-mediated regulation of DNA dosage in the ciliate *Oxytricha*. RNA. 2018 Jan;24(1):18-29. doi: 10.1261/rna.061333.117. Epub 2017 Oct 27. PMID: 29079634; PMCID: PMC5733567.

Krupina K, Goginashvili A, Cleveland DW. Causes and consequences of micronuclei. Curr Opin Cell Biol. 2021 Jun;70:91-99. doi: 10.1016/j.ceb.2021.01.004. Epub 2021 Feb 18. PMID: 33610905; PMCID: PMC8119331.
Lee SR, Pollard DA, Galati DF, Kelly ML, Miller B, Mong C, Morris MN, Roberts-Nygren K, Kapler GM, Zinkgraf M, Dang HQ, Branham E, Sasser J, Tessier E, Yoshiyama C, Matsumoto M, Turman G. Disruption of a ~23-24 nucleotide small RNA pathway elevates DNA damage responses in *Tetrahymena thermophila*. Mol Biol Cell. 2021 Jul 15;32(15):1335-1346. doi: 10.1091/mbc.E20-10-0631. Epub 2021 May 19. PMID: 34010017.
Marsh TC, Cole ES, Stuart KR, Campbell C, Romero DP. RAD51 is required for propagation of the germinal nucleus in Tetrahymena thermophila. Genetics. 2000 Apr;154(4):1587-96. doi: 10.1093/genetics/154.4.1587. PMID: 10747055; PMCID: PMC1461009.
Noto T, Kataoka K, Suhren JH, Hayashi A, Woolcock KJ, Gorovsky MA, Mochizuki K. Small-RNA-Mediated Genome-wide trans-Recognition Network in Tetrahymena DNA Elimination. Mol Cell. 2015 Jul 16;59(2):229-42. doi: 10.1016/j.molcel.2015.05.024. Epub 2015 Jun 18. PMID: 26095658; PMCID: PMC4518040.
Rzeszutek I, Maurer-Alcalá XX, Nowacki M. Programmed genome rearrangements in ciliates. Cell Mol Life Sci. 2020 Nov;77(22):4615-4629. doi: 10.1007/s00018-020-03555-2. Epub 2020 May 27. PMID: 32462406; PMCID: PMC7599177.
Song X, Gjoneska E, Ren Q, Taverna SD, Allis CD, Gorovsky MA. Phosphorylation of the SQ H2A.X motif is required for proper meiosis and mitosis in Tetrahymena thermophila. Mol Cell Biol. 2007 Apr;27(7):2648-60. doi: 10.1128/MCB.01910-06. Epub 2007 Jan 22. PMID: 17242195; PMCID: PMC1899910.
Swarts DC, Makarova K, Wang Y, Nakanishi K, Ketting RF, Koonin EV, Patel DJ, van der Oost J. The evolutionary journey of Argonaute proteins. Nat Struct Mol Biol. 2014 Sep;21(9):743-53. doi: 10.1038/nsmb.2879. PMID: 25192263; PMCID: PMC4691850.